Submillimeter-wave spectra of hypoiodous acid

Submillimeter-wave spectra of hypoiodous acid

Hiroyuki Ozeki
ISS Science Project Office, Japan Aerospace Exploration Agency, Tsukuba Space Center, 2-1-1 Sengen, Tsukuba 305-8585, Japan

Shuji Saito
Research Center for Development of Far-Infrared Region, Fukui University, 3-9-1 Bunkyo, Fukui 910-8507, Japan

Pure rotational spectra of hypoiodous acid, HOI, and its deuterated species, DOI, were measured in the frequency range of 320–670 GHz. The molecule was efficiently produced by a reaction of atomic oxygen with iodoethane. Rotational constants and centrifugal distortion constants for the molecule were determined accurately. The vibrationally averaged structure for HOI was obtained by taking the isotopic difference of the OH bond length into consideration: $r_z(\mathrm{OH}) = 0.967(8)$ Å, $r_z(\mathrm{OI}) = 1.9941(3)$ Å, and $\theta_z(\mathrm{HOI}) = 103.89°$, where the errors were estimated from the residual inertial defect. Equilibrium bond lengths for the OH and OI bonds were derived as 0.959(8) Å and 1.9874(3) Å, respectively, by assuming anharmonic constants of the corresponding diatomic molecules. Electric-quadrupole interaction constants and nuclear-spin–rotation coupling constants for the iodine nucleus were obtained. Nonaxial terms of the electric-quadrupole constant for HOI can be determined as well, which enabled us to derive the principal values of the coupling tensor. The values obtained were used to gauge the ionicity of the X–O bond in the HOX molecular system. The nuclear-spin-rotation coupling constant along the a inertial axis is found to be significantly smaller than others, which may be explained by a contribution from two low-lying singlet excited states.

I. INTRODUCTION

Hypoiodous acid, HOI, is one of the members of the hypohalous acids, HOX, where X=F, Cl, Br, and I. Among these species, HOCl and HOBr are widely known to be particularly important in the catalytic ozone destruction reactions in the stratosphere dubbed as ClOx, BrOx, or HOx cycles.[1] While it has been suggested that the HOI molecule can be linked to these three catalytic reaction cycles in the stratosphere and can play some roles in the troposphere as well (Refs. 2–6), their details have not yet been fully revealed. One of the reasons for this is incompleteness of the spectroscopic characterization of the molecule, as the lack of spectroscopic information can be an obstacle in conducting observations of the species in the actual atmosphere or in a laboratory. Gas-phase high-resolution spectroscopy of hypohalous acids has been reported mainly for HOF (Refs. 7–12), HOCl (Refs. 13–24), and HOBr (Refs. 25–28): thus, their molecular structures, harmonic force fields, dipole moments, and hyperfine coupling constants have been investigated in detail up to the present day. It is not the case, however, for the HOI molecule due to the paucity of relevant experimental works.

Formation of the HOI molecule in the laboratory condition was identified by Ogilvie *et al.* in 1975 (Ref. 29), with the detection of the hydrogen-bonded complex H_2CO-HOI by UV photolysis of a low-temperature matrix mixture of CH_3I and O_2. A clearer identification of the molecule was later made with assignments of three fundamental vibrational modes in the N_2 and Ar matrices by Walker *et al.*[30] They used *in situ* photolysis of a mixture of O_3 and HI to expect the O+HI reaction. Gas-phase identification of the HOI molecule was done by Barnes *et al.* with low-resolution (1 cm^{-1}) Fourier transform (FT) IR absorption spectroscopy.[31] They tried several reactions of OH radicals with I_2, CH_3I, or CH_2I_2 to form HOI: the maximum absorbance they obtained was 6% despite a White-type absorption cell with optical path length of 492 m being employed. They claimed as a conclusion that the lifetime of the molecule was too short in their experimental conditions for detailed studies. More recently, Loomis *et al.* found that vibrationally hot HOI was generated effectively by the reaction between atomic oxygen (^3P) and alkyl iodide ($C_nH_{2n+1}I$) with its alkyl chain of two carbon lengths or greater.[32] The reaction mechanism was investigated experimentally[33–36] as well as theoretically.[37] These studies have revealed that the reactions are all highly exothermic by approximately -240 kJ mol^{-1}, and more than 50% of the reaction exothermicity is deposited into the O–H stretch mode in relation to the fact that the reaction occurs through a novel five-membered ring intermediate.[36,37] This made it possible to observe the partially resolved vibration–rotation spectrum in emission with an FT-IR spectrometer (0.031 cm^{-1} apodized), and rotational constants in both the ground and ν_1 excited states (O–H stretching mode) for HOI and DOI were obtained.[38]

This paper reports the pure rotational spectra of the HOI and DOI molecules, resolving the hyperfine structure due to

the iodine nucleus. Interaction parameters for both the electric-quadrupole coupling and nuclear-spin–rotation coupling were obtained. A comparison of the molecular structure as well as the obtained hyperfine coupling constants with those of other hypohalous acids analogous is discussed.

II. EXPERIMENT

A 100-kHz-source-modulated submillimeter-wave spectrometer with a 1-m free-space cell was used to detect the HOI molecule. The details of the apparatus are essentially the same as previously reported.[39] The HOI molecule was generated by a reaction between iodoethane (C_2H_5I) and the oxygen atom, the latter being produced by a microwave discharge of O_2 with an Evenson-type microwave discharge cavity.[40] Both precursor gases were separately introduced to the free-space cell via side arms and were mixed at the upstream of the free-space cell. The reactant gas was evacuated from the downstream of the cell with a mechanical booster pump followed by a rotary pump.

With the aid of the molecular constants for HOI previously obtained by FT-IR work (Ref. 38), the initial spectral survey was started at the 363-GHz frequency region, where the one of the P branch transitions, $14_{114}-15_{015}$, was expected to occur. We found several lines 80 MHz below the prediction, which were split over 10 MHz presumably due to the electric-quadrupole interaction of the iodine nucleus. These lines appeared only when the microwave discharge was applied. We searched other transitions by revising the A rotational constant after optimization of the production efficiency at room temperature and found lines showing the same behavior very close to the frequencies predicted from the updated constants. Thus assignment of the spectra has been established: however, some of the lines were found to be disturbed by plenty of the lines due to other species. This difficulty was virtually solved by cooling the free-space cell to less than $-150\,^{\circ}C$. The HOI molecule was produced by reacting $O(^3P)$ with C_2H_5I upstream of the free-space cell and the product reacted immediately with other molecule to decompose. A cooled wall of the cell worked as a trap for unnecessary species, which made us to observe spectral lines of HOI without other disturbing lines. The optimum conditions for the production were partial pressures of C_2H_5I and O_2 to be 2.2 and 3.0 Pa, respectively, and a microwave discharge power of 40 W. The temperature of the cell was kept at $-150\,^{\circ}C$. We have tried to use methyl iodide (CH_3I) instead of C_2H_5I and found that the production efficiency of the HOI molecule is 5 times better when using C_2H_5I than CH_3I. For the production of DOI, deuterated iodoethane (C_2D_5I) was employed.

Spectral measurements were made over the frequency region of 320–670 GHz, resulting in the detection and identification of 215 and 100 spectral lines for HOI and DOI, respectively. Though both a- and b-type transitions were observed for HOI, we observed only b-type transitions for the DOI molecule which will be discussed later. Each line frequency was determined by averaging five pairs of upward and downward frequency-sweep measurements. The frequency measurement error was estimated to be between 30 and 120 kHz, depending on the spectral lines, or 60 kHz on average. An example of the observed spectra is shown in Fig. 1, and the selections of the observed transition frequencies are listed in Table I.[41]

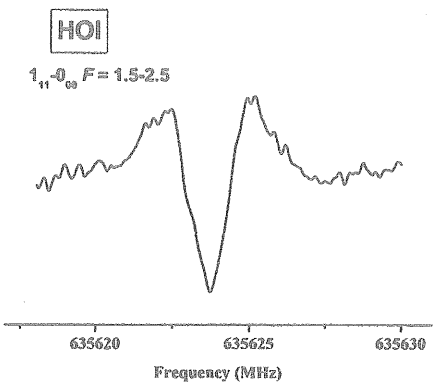

FIG. 1. An example of the observed spectra of HOI. The line corresponds to one of the hyperfine component ($F=1.5-2.5$) of the $1_{11}-0_{00}$ rotational transition. The spectrum was taken with an accumulation time of 12 s.

III. ANALYSIS

The observed spectral lines were analyzed using the following S-reduced Hamiltonian for an asymmetric top molecule:

$$H=H_{\rm rot}+H_{\rm eQq}+H_{\rm nsr}, \tag{1}$$

where $H_{\rm rot}$ represents the rotational Hamiltonian including the centrifugal distortion effect. $H_{\rm eQq}$ and $H_{\rm nsr}$ denote the Hamiltonians for an electric-quadrupole interaction and nuclear-spin–rotation interaction for the iodine nucleus, respectively. The matrix elements of the Hamiltonian were derived by using the standard method[42] with the basis function of $|NKI(\mathrm{I})FM_F\rangle$, employing the coupling scheme of $N+I(\mathrm{I})=F$ with $I(\mathrm{I})=5/2$. The energy levels were calculated by diagonalization of the Hamiltonian matrices. Among the observed spectral lines, 182 and 91 line frequencies were subjected to a least-squares fit to determine the molecular constants for HOI and DOI, respectively, which correspond approximately to 90% of the whole observed lines. The line frequencies showing the obs–calc value being more than 90 kHz were not used in the present fit. The frequency of the blended line was directly compared with a calculated value which was averaged for the calculated frequencies of the component lines weighted by their relative intensities. We estimated hyperfine coupling constants on the basis of the values of HOBr (Ref. 25), BrO (Ref. 43), and IO (Ref. 44) in order to use them as initial values of the fit. As a result, the agreement between observed and calculated hyperfine pattern is satisfactory with respect to line frequency as well as relative intensity, as depicted in Fig. 2. The D_K constant was not possible to be floated because all the observed b-type transitions in the present work were designated to $K_a=1-0$, and the latter was fixed at 171.7 MHz for HOI as obtained in the FT-IR study.[38] Since the corresponding constant for the DOI molecule was not available by the previous works, it was estimated by assuming a diatomic

TABLE I. Selection of the observed and calculated transition frequencies of HOI and DOI in MHz.

Transition	$F'-F''$	HOI	DOI
$4_{14}-5_{05}$	2.5–2.5	535299.191(−111)[a,b]	
	3.5–3.5	535366.982(−37)	
	4.5–4.5	535495.175(−9)	
	6.5–7.5	535554.603(−22)	251616.774(87)
	1.5–2.5	535569.765(−64)	
	4.5–5.5		251723.385(45)
	5.5–6.5	535618.317(−20)	
	2.5–3.5	535642.820(−5)	
	4.5–3.5	535662.071(45)	251734.426(−13)
	3.5–4.5	535672.997(31)	
	5.5–5.5	535715.517(−3)	
	6.5–6.5	536066.295(−27)	
$3_{13}-4_{04}$	2.5–2.5	552239.656(19)	
	3.5–3.5	552351.390(−1)	267408.267(15)
	5.5–6.5	552380.908(35)	267438.226(30)
	0.5–1.5	552384.920(−41)	267442.682(6)
	4.5–5.5	552497.141(20)	267553.861(−2)
	1.5–2.5	552500.164(−63)	267557.396(−73)
	3.5–4.5	552558.585(45)[c]	
	4.5–5.5		
	2.5–3.5	552560.809(22)	267617.558(21)
	5.5–5.5		267960.978
$1_{10}-1_{01}$	1.5–1.5		329444.958(−64)
	3.5–3.5	619112.027(−58)	329849.558(−6)
	2.5–1.5	619161.245(78)	329899.093(−5)
	2.5–3.5	619428.882(−47)	330166.479(8)
	1.5–2.5	619594.247(−19)	330330.161(−15)
	3.5–2.5	619731.478(121)[b]	330467.327(−18)
	2.5–2.5		330784.227(−25)
$2_{11}-2_{02}$	3.5–4.5	619072.326(72)	329881.230(−19)
	2.5–1.5	619141.044(−51)	329949.473(42)
	4.5–4.5	619347.035(72)	330154.332(−14)
	2.5–2.5		33364.278(39)
	3.5–2.5	619487.398(18)	
	3.5–3.5	619641.652(−202)[b]	330449.516(−11)
	2.5–3.5	619711.786(97)	330518.886(−7)
	1.5–2.5	619770.694(−44)	330577.399(121)[a]
	4.5–3.5		330722.573(−52)
	2.5–1.5		329949.473(42)
$1_{11}-0_{00}$	1.5–2.5	635624.641(66)	345154.482(−29)
	3.5–2.5	635757.778(−84)	345287.320(−33)
	2.5–2.5	636065.789(−69)	345594.294(34)
$2_{12}-1_{01}$	2.5–1.5	651801.534(−17)	360124.841(18)
	3.5–3.5	651997.258(−95)	360320.372(−55)
	1.5–1.5	652021.079(−3)	360344.742(44)
	0.5–1.5	652206.647(−53)	
	4.5–3.5	652280.270(72)	360602.714(23)
	3.5–2.5	652616.552(−73)	360938.207(−1)
	2.5–2.5	652688.650(64)	361010.024(47)

[a]Values in parentheses denote observed and calculated frequencies in kHz.
[b]Not included in the fit.
[c]Blended line.

approximation.[45] The standard deviations of the fits were 46 and 35 kHz for HOI and DOI, respectively, where the same weights were applied for all data included in the fit. The calculated frequencies and the derived molecular constants are summarized in Table I and II, respectively.

The rotational constants for HOI determined in the present study compare well with the previous FT-IR result[38] as seen in Table II. While the A and B constants were found to be deviated by 5 times the quoted errors in the previous study, the C constant almost coincides with ours. These

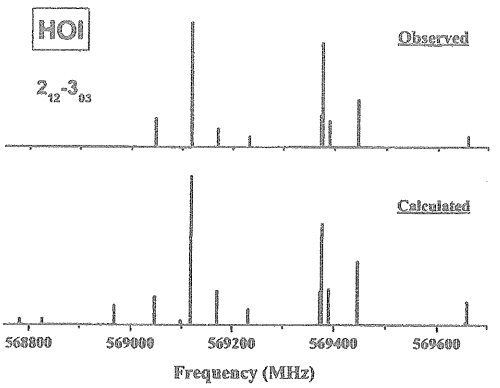

FIG. 2. Observed (upper panel) and calculated (lower panel) hyperfine spectral patterns for the 2_{12}–3_{03} transition of HOI.

agreements made our initial spectral assignment easier. The rotational constants for the DOI molecule were obtained. The hyperfine splitting patterns were basically explained well by using the axial components of the interaction tensor for both the electric-quadrupole interaction and nuclear-spin–rotation interaction. In addition, we found that nonaxial component of the electric-quadrupole coupling tensor χ_{ab}(I) was significantly determined for HOI, though it has a large uncertainty.

IV. DISCUSSION

We obtained rotational constants for both HOI and DOI, with which the effective molecular structure can be calculated—i.e., r_0(OH)=0.957(21) Å, r_0(OI)=1.9926 (8) Å, and θ_0(HOI)=103.94(45)°, where the errors come from the inertial defect. Three structural parameters have been determined independently, while the OH bond length

TABLE II. Molecular constants of HOI and DOI in MHz.

	HOI		DOI
Constant	Present Work	FT-IR[a]	Present work
A	627757.3727(151)[b]	627608.(98)	337768.379(22)
B	8366.22250(179)	8362.4(26)	7831.0217(89)
C	8246.4307(23)	8246.4(24)	7642.3548(58)
D_J	0.0077207(23)	0.00707(28)	0.00682(20)
D_{JK}	0.618704(116)	0.601(28)	0.33094(197)
D_K	171.7(fixed)[c]	171.7(74)	50.(fixed)[d]
d_1	0.00009804(51)	−0.00056(58)	−0.0001464(29)
d_2	−0.00000518(69)		
H_{JKK}	0.0007405(172)		
χ_{aa}(I)	−2951.982(170)		−2945.294(170)
χ_{bb}(I)	1454.864(111)		1448.808(137)
χ_{ab}(I)	−169.(76)		
C_{aa}(I)	0.0117(186)		0.0105(197)
C_{bb}(I)	0.0711(41)		0.0647(52)
C_{cc}(I)	0.0623(49)		0.0551(54)

[a]Reference 38. The constants were originally given in the unit of cm^{-1} and were converted to MHz.
[b]Values in parentheses denote three times standard deviation and apply to the last digits.
[c]Fixed to the value obtained by FT-IR (Ref. 38).
[d]Estimated by assuming diatomic approximation.

was assumed to be the same as that of HOBr and HOCl in previous FT-IR work.[38] The OI bond and a inertial axis make an angle of approximately 1.79° for HOI, and it increases by 1.57° upon deuterization. In the present study we have observed both a- and b-type transitions for HOI, but only the b-type transition was successful to observe for DOI. This can be explained by considering that the composite direction of the permanent dipole is almost parallel to the b inertial axis, and the amount of projection onto the a axis is sensitive to inertial axis rotation. Our spectral intensity measurements suggested that the ratio for the dipole moments $(\mu_b/\mu_a)^2$ is estimated to be 25 for HOI and more than 100 for DOI.

The inertial defect of the molecule is calculated to be $\Delta_0 = 0.072\,449(22)$ uÅ^2 for HOI, which is slightly different from the previous one, $\Delta_0 = 0.045(8)$ uÅ^2 (Ref. 38). The inertial defects of other hypohalous acids were reported to be 0.059 190(15), 0.063 9119(64), and 0.067 175(16) uÅ^2, for HOF (Ref. 11), HO^{35}Cl (Ref. 22), and HO^{79}Br (Ref. 27), respectively. Our result seems to be consistent with them as the values increase monotonically from the fluorine analogous to the iodine one. The inertial defect Δ_0 can be expressed by the sum of three factors:[46]

$$\Delta_0 = \Delta_{\text{vib}} + \Delta_{\text{cent}} + \Delta_{\text{elec}}. \tag{2}$$

The vibrational contribution Δ_{vib} is the most important among the three, and Herschbach and Laurie proposed a simple approximation for calculating Δ_{vib}, in which the major part of it can attribute to the lowest in-plane vibration.[47] In the case of hypohalous acids, the inertial defect is thus inversely proportional to the vibrational frequency of the ν_3 mode, which is the O–X stretching, where X denotes the corresponding halogen atom. The observed fundamental frequencies of the ν_3 mode are 889.079 74, 724.358 07, 620.18, and 575 cm^{-1}, for HOF (Ref. 10), HO^{35}Cl (Ref. 19), HO^{79}Br (Ref. 26), and HOI (Ref. 30), respectively. Therefore, qualitative explanation can be given by the approximate relation described above.

The harmonic force field of the HOI molecule can be derived from centrifugal distortion constants and vibrational frequencies. If we employ internal coordinates of the molecule, S_1, S_2, and S_3, to be Δr(OH), Δr(OI), and $\Delta\theta$(HOI), respectively, then diagonal components among six independent force constants are f_{11} (OH stretch), f_{22} (OI stretch), and f_{33} (HOI bend). Computation was performed by the ASYM40 package coded by Hedberg and Mills,[48,49] and the results are summarized in Tables III and IV. As can be seen in the table, the errors for the vibrational frequencies are estimated by taking the matrix shift and anharmonic contribution into account. With the aid of the harmonic force field thus obtained, the vibrational average structure (r_z) can be estimated from the vibrational averaged constants B_z, which are obtained by correcting the observed rotational constants B_0 for harmonic vibrational effects.[50–53] The calculated values for B_z are listed in Table V, showing small residual inertial defects. This makes the systematic error in deriving the molecular structure smaller. The isotopic difference of the bond length Δr_z was estimated as well, which shows a sizable difference between OH and OD bonds as a result of anharmonicity. The Δr_z value can be assessed with a diatomic approximation as the following formula:[54]

$$\Delta r_z = \frac{3}{2} a_3 \Delta\langle \Delta z^2 \rangle - \frac{\Delta(\langle \Delta x^2 \rangle + \langle \Delta y^2 \rangle)}{2 r_e}, \tag{3}$$

where Δx, Δy, and Δz are displacements of local Cartesian coordinates, and a_3 and r_e denote the third-order anharmonic constants for the OH bond and equilibrium bond length, respectively. $\Delta\langle\cdots\rangle$ refers to the difference of the average value in question between OH and OD bonds. In this case the z axis is taken to be that which lies along the OH(OD) bond. The a_3 value is assumed to be the same for the OH molecule, 2.332 Å^{-1}, as listed in the table compiled by Kuchitsu *et al.*[54] The Δr_z value can be calculated to be 0.0023 Å, which compares well with the HOCl/DOCl system estimated by Anderson *et al.*,[18] suggesting the validity of the present

TABLE III. Observed and calculated centrifugal distortion constants and vibrational wave numbers of HOI.

	HOI		DOI	
	Observed	Calculated	Observed	Calculated
D_J[a]	7.7207(23)	7.7229	6.82(20)	6.37
D_{JK}	618.704(116)	618.649	330.94(197)	350.89
D_K	171700[c]	153200.	50000.[c]	48000
d_1	−0.09804(51)	−0.0897	−0.1464(29)	−0.137
d_2	−0.00518(69)	−0.0042		−0.011
ω_1[b]	3625.84(500)[d]	3627.	2653.(20)[f]	2641.
ω_2	1068.(5)[e]	1051.	808.(20)[f]	759.
ω_3	575.(20)[f]	568.	571.(20)[f]	563.

[a]Units are in kHz.
[b]Units are in cm^{-1}.
[c]Not included in the fit as the constants was not derived directly from the present work.
[d]Reference 38. Estimated error due to anharmonicity.
[e]Reference 31. Estimated error due to anharmonicity.
[f]Reference 30. Estimated error due to matrix shift and anharmonicity.

TABLE IV. Harmonic force field for HOI.[a]

Force constant	
f_{11} (aJ Å^{-2})	7.34(13)
f_{22} (aJ Å^{-2})	2.963(16)
f_{23} (aJ Å^{-2} rad^{-1})	0.372(27)
f_{33} (aJ rad^{-2})	0.570(35)

[a]The internal coordinates used are $S_1 = \Delta r$(OH), $S_2 = \Delta r$(OI), and $S_3 = \Delta\theta$(HOI). The effective structure (r_0) was used for the geometry—i.e., r(OH) = 0.957 Å, r(OI) = 1.9926 Å, and θ(HOI) = 103.94°. f_{12} and f_{13} were fixed to 0.

TABLE V. Vibrational averaged constants for HOI and DOI.

	HOI	DOI
A_z[a]	614408.0	332178.
B_z	8347.67	7812.72
C_z	8235.55	7633.17
Δ_z[b]	0.00167	0.00017

[a]Units are in MHz.
[b]Units are in uÅ^2.

TABLE VI. Molecular structure for HOI.

	r(OH) (Å)	r(OI) (Å)	θ(HOI) (deg)
Expt. (r_z)[a]	0.967(8)	1.9941(3)	103.89(20)
Expt. (r_e)[a]	0.959(8)	1.9874(3)	103.89[b]
Expt. (r_0)[c]	0.964[d]	1.991	105.4
Calc. (B3LYP)[e]	0.964	2.000	106.1
Calc. (MP2)[e]	0.964	1.984	104.8

[a]Present work.
[b]Assumed to be equal to θ_z(HOI).
[c]Reference 38.
[d]The OH bond length is assumed to the same as that of HOBr and HOCl.
[e]Reference 55.

estimation. Then the r_z structure is derived from the six corrected constants with the boundary condition of the isotopic difference of the OH bond length: i.e., r_z(OH) $=0.967(8)$ Å, r_z(OI) $=1.9941(3)$ Å, and θ_z(HOI) $=103.89(20)°$. Here we assumed common values for r_z(OI) and θ_z(HOI) among isotopomers, and the errors in the parentheses were estimated from residual inertial defects.

The equilibrium bond distance can be evaluated from the vibrationally averaged structure:[54]

$$r_e = r_z - \frac{3}{2}a_3\langle\Delta z^2\rangle + \frac{(\langle\Delta x^2\rangle + \langle\Delta y^2\rangle)}{2r_e}. \quad (4)$$

The r_e distances for the OH and OI bond lengths are derived to be 0.959(8) Å and 1.9874(3) Å, respectively. The estimated structures of hypoiodous acid are summarized in Table VI together with the results of the latest *ab initio* calculations.[55] Agreements between the present result (r_e) and that by MP2 calculation are satisfactory, while the density functional theory (DFT) calculation overestimated the OI bond length.

The hyperfine structure due to the iodine nucleus has been resolved and the corresponding parameters were determined. Electric-quadrupole coupling constants for hypohalous acids are summarized in Table VII. Since the nonaxial component $\chi_{ab}(\mathrm{I})$ has been determined in the present study,

TABLE VII. Comparison of electric-quadrupole coupling constants in MHz.

	HOI[a]	HO^{79}Br[b]	HO^{35}Cl[c]
$\chi_{aa}(X)$[d]	−2951.982(170)[e]	915.663(57)	−121.958(24)
$\chi_{bb}(X)$	1454.864(111)	−448.905(48)	59.519(30)
$\chi_{cc}(X)$	1497.118(111)	−466.758(48)	62.439(30)
$\chi_{ab}(X)$	−169.(76)	20.4(24)[f]	
$\chi_{xx}(X)$	1461.3(60)	−450.58	
$\chi_{yy}(X)$	1497.1(60)	−466.76	
$\chi_{zz}(X)$	−2958.4(60)	917.34	
$\chi_z(X)$	−3698.0	1146.7	−152.4[g]
$eQq_{n10}(X)$[h]	2292.71	−769.76	109.74
i_c	0.50	0.40	0.32
$\Delta(\chi_O-\chi_X)$[h]	0.9	0.6	0.4

[a]Present work.
[b]Reference 25.
[c]Reference 16.
[d]X denotes halogen nucleus of the corresponding molecule.
[e]Values in parentheses denote 3σ error and apply to the last digits.
[f]Derived from the diagonal constants of the isotopomers.
[g]$\chi_{zz}(X)=\chi_{aa}(X)$ is assumed.
[h]Reference 58.

we can estimate principal values in the quadrupole tensor axis system. This will be accomplished by rotating the inertial axis frame within the molecular plane toward the O–I bond by 2.19(98)°, where the error comes from those of the molecular constants obtained. The $\chi_{zz}(\mathrm{I})$ is thus estimated to be −2958.4(60) MHz. The contribution from unbalanced p electrons, $\chi_z(\mathrm{I})$, is derived from $\chi_{zz}(\mathrm{I})$, by taking the electron angular distribution into account, to be −3698.0 MHz. This value can be directly compared with the atomic value. In hypohalous acid molecules except for HOF, a positive pole is considered to be on the halogen atom. For such cases, the quadrupole coupling due to an unbalanced p electron of the halogen atom is given by the formula

$$\chi_z(X) = -(1+i_c)(1-a_s^2)(1+i_c\varepsilon)eQq_{n10}(X), \quad (5)$$

where i_c, a_s, and ε denote the ionicity and degree of s hybridization of the XO bond and screening constants, respectively. If we do not account for s hybridization and take a typical screening constants for halogen atom ($\varepsilon=0.15$), then the ionicity of the XO bond can be evaluated. The results are listed in Table VII, showing that the values increase from hypochlorous acid to hypoiodous acid. This is consistent with the difference of electronegativity of the atoms making the XO bond, $\Delta(\chi_O-\chi_X)$, inferring that the contribution from the ionic structure, HO^-X^+, becomes larger as X is varied from the chlorine atom to the iodine atom. Interestingly, r_e(OH) obtained in the present study [0.959(8) Å] shows a very close value to the one for r_e(OH) [0.964 317(22) Å].[56,57]

Nuclear-spin–rotation coupling constants can be effectively expressed as the sum of the positive and negative contributors, which are the second-order correction to the electronic energy due to excitation of the valence electrons by rotation and the effect of the nuclear charges—i.e., the slippage of electrons with respect nuclei.[58] Except for the hydrogen nucleus, however, the first term usually dominates, so that the constant C_{ii} can be expressed effectively as

$$C_{ii} = 4B_{ii}\sum_n \frac{a_{0n}|\langle 0|L_i|n\rangle|^2}{E_n - E_0},$$

where B_{ii} denotes the rotational constants, a_{0n} the off-diagonal nuclear-spin–orbit interaction constant, L_i the i component of the orbital angular momentum, and E_n and E_0 the unperturbed electronic energy of the nth excited and ground states, respectively. Thus the value projected onto the a inertial axis can be the largest among the three elements because of the largest rotational constant. However, the derived C_{aa} constant in the present study shows the smallest value. The electronic configuration of the ground state HOI at the Hartree–Fock level can be expressed as follows:[59]

$$1\,^1A'(\mathrm{HOI}) = (\mathrm{core})^{48}(18a')^2(19a')^2(20a')^2(8a'')^2 \times (21a')^2(22a')^2(9a'')^2(23a')^0.$$

The first and second singlet electronic excited states, $1\,^1A''$, and $2\,^1A$ can be well designated by the excitation of $(9a'') \rightarrow (23a')$ and $(22a') \rightarrow (23a')$, respectively. We focus on the two lowest excited states in the discussion, because the contributions from these excited states will be dominant due

TABLE VIII. Comparison of the nuclear-spin–rotation coupling constants.

	HOI[a]	DOI[a]	$HO^{79}Br$[b]	$HO^{81}Br$[b]	$DO^{79}Br$[b]	$DO^{81}Br$[b]	$HO_{35}Cl$[c]
$C_{aa}(X)$[d]	11.7(186)[e]	10.5(197)	50.(60)	−32.(65)	15.(16)	29.(16)	−3.8(28)
$C_{bb}(X)$	71.1(41)	64.7(52)	60.8(14)	64.0(13)	57.6(14)	61.2(14)	−19.(2)
$C_{cc}(X)$	62.3(49)	55.1(54)	55.8(14)	59.9(13)	52.6(14)	54.9(14)	0.9(20)
$\Lambda_{aa}(X)$[f]	0.0066(105)	0.011(21)	0.039(48)	−0.023(47)	0.022(23)	0.039(22)	−0.0075(56)
$\Lambda_{bb}(X)$	3.027(175)	2.94(24)	2.73(6)	2.68(5)	2.75(7)	2.73(6)	−0.82(9)
$\Lambda_{cc}(X)$	2.69(21)	2.57(25)	2.55(6)	2.55(6)	2.60(7)	2.52(6)	0.07(17)

[a]Present work.
[b]Reference 25.
[c]Reference 16.
[d]Units are in kHz. X denotes halogen nucleus of the corresponding molecule.
[e]Values in parentheses denote 3σ error and apply to the last digits.
[f]Values are multiplied by 10^6.

to the smaller energy differences $E_n - E_0$. The first excited state ($1\,^1A''$) should be coupled with the angular momentum operator of L_a or L_b, and the second one ($2\,^1A'$) with that of L_c from symmetry considerations. There are no theoretical predictions specifically for the properties of any excited electronic states of HOI. In the analogy with other hypohalous acids, the characters of the orbitals relating to the electronic excitation will be the following:[60–63]

$22a'$: nonbonding iodine p orbital in the molecular plane,

$9a''$: OI π antibonding(π^*_{OI}),

$23a'$: OI σ antibonding (σ^*_{OI}).

Given this information, it might be possible to give a qualitative explanation for the extraordinary value of C_{aa} by evaluation of the matrix element of the orbital angular momentum.[64] For the σ^*_{OI} orbital ($23a'$), the positive lobes at O and I sites both point toward the same direction along the OI bond. In this case the OI bond almost coincides with the a principal axis, so that the directions are both regarded as $+a$. On the contrary, the positive lobes of the $9a''$ orbital point in the opposite direction at the O and I sites—i.e., $+c$ at the I atom and $-c$ at the O atom, or vice versa. Therefore only the b component of the angular momentum can be generated. If we look toward the $+b$ direction, we find that the iodine-atom electronic angular momentum and that of the oxygen atom will be added or not be canceled with each other by considering a counterclockwise rotation. In the same way, the nonbonding p orbital ($22a'$) makes a perpendicular configuration with $23a'$, which generates the c component of the electronic angular momentum. Our qualitative interpretation may be applied to other hypohalous acids analogously. Evidently, we observe a similarity with respect to the magnitude of the constants for them shown in Table VIII, in which the value of $\Lambda_{ii} = C_{ii}/B_{ii}g_I$ was calculated to look at the trend. Here g_I is the nuclear g factor. All the Λ_{aa} values listed in the table are smaller by two orders of magnitude than other axis components, implying common properties of the electronic states of hypohalous acids.

ACKNOWLEDGMENT

The authors thank Takashi Imamura for valuable discussions.

[1] For example, B. J. Finlayson-Pitts and J. N. Pitts, Jr., *Chemistry of the Upper and Lower Atmosphere* (Academic, San Diego, 2000).
[2] W. L. Cameides and D. D. Davis, J. Geophys. Res. **85**, 7383 (1980).
[3] M. E. Jenkin, R. A. Cox, and D. E. Candeland, J. Atmos. Chem. **2**, 359 (1985).
[4] S. Solomon, R. R. Garcia, and A. R. Ravishankara, J. Geophys. Res. **99**, 20491 (1994).
[5] S. Solomon, J. B. Burkholder, A. R. Ravishankara, and R. R. Garcia, J. Geophys. Res. **99**, 20929 (1994).
[6] N. S. Holmes, J. W. Adams, and J. N. Crowley, Phys. Chem. Chem. Phys. **3**, 1679 (2001).
[7] H. Kim, E. F. Pearson, and E. H. Appleman, J. Chem. Phys. **56**, 1 (1972).
[8] E. F. Pearson and H. Kim, J. Chem. Phys. **57**, 4230 (1972).
[9] S. L. Rock, E. F. Pearson, E. H. Appleman, C. L. Norris, and W. H. Flygare, J. Chem. Phys. **59**, 3940 (1973).
[10] H. Bürger, G. Pawelke, S. Sommer, A. Rahner, E. H. Appleman, and I. M. Mills, J. Mol. Spectrosc. **128**, 278 (1988).
[11] H. Bürger, G. Pawelke, S. Sommer, A. Rahner, E. H. Appleman, and I. M. Mills, J. Mol. Spectrosc. **136**, 197 (1989).
[12] H. Bürger, G. Pawelke, A. Rahner, E. H. Appleman, and L. Halonen, J. Mol. Spectrosc. **138**, 346 (1989).
[13] M. Suzukiand and A. Guarnieri, Z. Naturforsch. A **30**, 497 (1975).
[14] J. S. Wells, R. L. Sams, and W. J. Lafferty, J. Mol. Spectrosc. **77**, 349 (1979).
[15] R. L. Sams and W. B. Olson, J. Mol. Spectrosc. **84**, 113 (1980).
[16] H. E. G. Singbeil, W. D. Anderson, R. W. Davis, M. C. L. Gerry, E. A. Cohen, H. M. Pickett, F. J. Lovas, and R. D. Suenram, J. Mol. Spectrosc. **103**, 466 (1984).
[17] C. M. Deely and I. M. Mills, J. Mol. Spectrosc. **114**, 368 (1985).
[18] W. D. Anderson, M. C. L. Gerry, and R. W. Davis, J. Mol. Spectrosc. **115**, 117 (1986).
[19] W. J. Lafferty and W. B. Olson, J. Mol. Spectrosc. **120**, 359 (1986).
[20] C. M. Deely, J. Mol. Spectrosc. **122**, 481 (1987).
[21] M. Carlotti, G. D. Lonardo, L. Fusina, and A. Trombetti, J. Mol. Spectrosc. **141**, 29 (1990).
[22] M.-L. Junttila, W. J. Lafferty, and J. B. Burkholder, J. Mol. Spectrosc. **164**, 583 (1994).
[23] C. Azzolini, F. Cavazza, G. Crovetti, G. D. Lonardo, R. Frulla, R. Escribano, and L. Fusina, J. Mol. Spectrosc. **168**, 494 (1994).
[24] M. Brillini, P. D. Natale, L. Fusina, and G. Modugno, J. Mol. Spectrosc. **172**, 559 (1995).
[25] Y. Koga, H. Takeo, S. Kondo, M. Sugie, C. Matsumura, G. A. McRae, and E. A. Cohen, J. Mol. Spectrosc. **138**, 467 (1989).
[26] G. A. McRae and E. A. Cohen, J. Mol. Spectrosc. **139**, 369 (1990).
[27] E. A. Cohen, G. A. McRae, T. L. Tan, R. R. Freidl, J. W. C. Johns, and M. Noel, J. Mol. Spectrosc. **173**, 55 (1995).
[28] T. L. Tan and K. L. Goh, J. Mol. Spectrosc. **199**, 87 (2000).

[29] J. F. Ogilvie, V. R. Salares, and M. J. Newlands, Can. J. Chem. **53**, 269 (1975).
[30] N. Walker, D. E. Tevault, and R. R. Smardzewski, J. Chem. Phys. **69**, 564 (1978).
[31] I. Barnes, K. H. Becker, and J. Starcke, Chem. Phys. Lett. **196**, 578 (1992).
[32] S. R. Leone, J. J. Klaassen, and J. Linder, in *Abstracts of Papers—American Chemical Society* (American Chemical Society, Washington, D.C., 1995), Pt. 2, p. 210.
[33] R. A. Loomis, J. J. Klaassen, J. Linder, P. G. Christopher, and S. R. Leone, J. Chem. Phys. **106**, 3934 (1996).
[34] J. J. Wang, D. J. Smith, and R. Grice, J. Phys. Chem. **100**, 13603 (1996).
[35] J. J. Wang, D. J. Smith, and R. Grice, J. Phys. Chem. **100**, 6620 (1996).
[36] R. A. Loomis, S. R. Leone, and M. K. Gilles, Res. Chem. Intermed. **24**, 707 (1998).
[37] J. E. Stevens, Q. Cui, and K. Morokuma, J. Chem. Phys. **108**, 1544 (1998).
[38] J. J. Klaassen, J. Linder, and S. R. Leone, J. Chem. Phys. **104**, 7403 (1996).
[39] S. Saito and M. Goto, Astrophys. J. Lett. **410**, L53 (1993).
[40] F. C. Fehsenfeld, K. M. Evenson, and H. P. Broida, Rev. Sci. Instrum. **36**, 294 (1965).
[41] See EPAPS Document No. E-JCPSA6-120-002411 for the observed and calculated transition frequencies for HOI. This document may be retrieved via the EPAPS homepage (http://www.aip.org/pubservs/epaps.html) or from ftp.aip.org in the directory /epaps/. See the EPAPS homepage for more information.
[42] A. R. Edmonds, *Angular Momentum in Quantum Mechanics* (Princeton University Press, Princeton, 1957).
[43] F. Tamassia, S. M. Kermode, and J. M. Brown, J. Mol. Spectrosc. **205**, 92 (2001).
[44] S. Saito, J. Mol. Spectrosc. **48**, 530 (1973).
[45] J. Demaison, M. LeGuennec, G. Wlordarczak, and B. P. Van Eijck, J. Mol. Spectrosc. **159**, 357 (1993).
[46] T. Oka and Y. Morino, J. Mol. Spectrosc. **6**, 472 (1961).
[47] D. R. Herschbach and V. W. Laurie, J. Chem. Phys. **40**, 3142 (1964).
[48] L. Hedberg and I. M. Mills, J. Mol. Spectrosc. **160**, 117 (1993).
[49] L. Hedberg and I. M. Mills, J. Mol. Spectrosc. **230**, 82 (2000).
[50] T. Oka, J. Phys. Soc. Jpn. **15**, 2274 (1960).
[51] M. Toyama, T. Oka, and Y. Morino, J. Mol. Spectrosc. **13**, 193 (1964).
[52] D. R. Herschbach and V. W. Laurie, J. Chem. Phys. **37**, 1668 (1962).
[53] V. W. Laurie and D. R. Herschbach, J. Chem. Phys. **37**, 1687 (1962).
[54] K. Kuchitsu, M. Nakata, and S. Yamamoto, in *Stereochemical Applications of Gas-phase Electron Diffraction*, edited by I. Hargittai and M. Hargittai (VCH, New York, 1988), pt. A.
[55] S. Berski, B. Silvi, Z. Latajka, and J. Leszczynski, J. Chem. Phys. **111**, 2542 (1999).
[56] D.-J. Liu and T. Oka, J. Chem. Phys. **84**, 2426 (1986).
[57] N. H. Rosenbaum, J. C. Owrutsky, L. M. Tack, and R. J. Saykally, J. Chem. Phys. **84**, 5308 (1986).
[58] C. H. Towns and A. L. Schawlow, *Microwave Spectroscopy* (Dover, New York, 1975).
[59] B. F. Minaev, J. Phys. Chem. A **103**, 7294 (1999).
[60] R. L. Jaffe and S. R. Langhoff, J. Chem. Phys. **68**, 1638 (1978).
[61] S. Nanbu and S. Iwata, Chem. Phys. **135**, 75 (1989).
[62] S. Nanbu and S. Iwata, J. Phys. Chem. **96**, 2103 (1992).
[63] M. Lock, R. J. Barnes, and A. Sinha, J. Phys. Chem. **100**, 7972 (1996).
[64] R. F. Curl, Jr., J. Chem. Phys. **37**, 779 (1962).